

# Energy-Efficient Massive IoT Shared Spectrum Access over UAV-enabled Cellular Networks

Ghaith Hattab, *Student Member, IEEE*, Danijela Cabric, *Senior Member, IEEE*

**Abstract**—Providing connectivity to a massive number of sensors and machines, commonly known as massive Internet-of-things (IoT), has become a critical use case for fifth-generation new radio (5G-NR). Nevertheless, existing transmission protocols, e.g., orthogonal allocation or spectrum sharing, can be detrimental for cellular users (UEs) and IoT devices due to increased congestion and interference or resource splitting. To this end, we consider to equip cellular networks with unmanned aerial vehicles (UAVs), e.g., drones, acting as mobile data aggregators. Specifically, we propose a transmission protocol for shared spectrum access between IoT devices and UEs, where IoT traffic is collected by drones and then aggregated to the cellular network. Using stochastic geometry, we analyze the performance of the proposed protocol and compare it with existing ones. In addition, we present a stochastic optimization framework that optimizes the transmit power of IoT devices to maximize the average energy-efficiency (EE) of a typical IoT device subject to interference constraints on UEs. Simulation results are presented to validate the effectiveness of the proposed transmission protocol and power control, showing significant improvements of the EE of IoT devices, and hence their lifetime, with minimal degradation on the UE spectral efficiency when compared to existing transmission schemes.

**Index Terms**—5G-NR, cellular networks, Internet-of-things, massive IoT, spectrum sharing, stochastic geometry, UAVs.

## I. INTRODUCTION

Fifth-generation new-radio (5G-NR) is set to unlock new application scenarios at different fronts. One specific use case is the native support of a massive number of sensors and machines, collectively known as massive cellular Internet-of-things (IoT) or massive machine-type communications (mMTC) [2]. Indeed, it is envisaged that billions of IoT devices will require Internet-connectivity by 2020, creating transformative economic potentials for operators and stakeholders, reaching trillions of dollars [3]. Further, the massive IoT market is expected to span many vertical sectors, including smart cities, public safety, and agriculture [4].

The support of IoT services over cellular networks is not new. For instance, recent LTE-A cellular standards, e.g., Rel. 13 and Rel. 14, have introduced new user categories tailored for IoT applications, e.g., CAT-0, CAT-M, and NB-IoT, in addition to enabling extended discontinuous reception (eDRX) to reduce power consumption [5], [6]. Such IoT optimizations, however, are still limited to services that do not require a large deployment of sensors and machines. Indeed, as the density of IoT devices increases, several challenges emerge [7]. First, collisions among IoT devices increase due to the

increased number of access requests, making retransmissions more frequent, and thus affecting their energy-efficiency (EE). Second, interference increases when IoT devices share the same spectrum with cellular users (UE), degrading the coverage needed for the former and reducing the spectral efficiency (SE) for the latter. For these reasons, our objective is to propose a transmission protocol that enables a harmonious coexistence of massive IoT with UEs over cellular networks.

## A. Related work

The techniques toward the coexistence of IoT devices and UEs can be broadly classified into two categories: orthogonal-based and sharing-based solutions [6], [7]. In the former, resource blocks are split among IoT devices and UEs either over time [8] or frequency [9], [10] as means to avoid interference and congestion. However, resource partitioning inevitably leads to a spectral efficiency tradeoff between IoT devices and UEs. In contrast, in spectrum sharing, all resource blocks are shared between UEs and IoT devices. To control congestion, several techniques have emerged such as access class barring (ACB) and randomized back-off schemes [11]–[13]. These methods, nevertheless, do not address the co-channel interference after access requests are granted. Alternative to these approaches, data aggregation has emerged as an effective solution to handle the massive IoT traffic. An experimental study is discussed in [4] showing the benefits of IoT data aggregation on cellular networks. In [14]–[17], stochastic geometry is used to analyze the coverage performance and/or the energy consumption using single and/or multiple aggregators. These works, however, consider fixed terrestrial aggregators and focus only on the performance of IoT devices, i.e., the coexistence of IoT devices and UEs is not considered. In this paper, we consider using unmanned aerial vehicles (UAVs) or drones that stop at optimized predetermined locations.

Integrating UAVs with cellular networks has attracted significant attention, e.g., it has become a study item for recent and future 3GPP releases [18]. Indeed, UAVs are envisioned to become data aggregators (relays) or even base stations (BSs) [19], as their mobility brings unparalleled flexibility to cellular networks. For example, UAVs can help realize several IoT applications, e.g., smart cities, by extending the coverage of existing cellular infrastructure, enabling low-power communications with low-cost sensors, and reducing network congestion via offloading some of the traffic generated from massive IoT devices [20]. Implementation and practical considerations for UAV-based IoT platforms are presented in [21]–[23], showing the feasibility of using UAVs for IoT

This paper was presented in part at the IEEE Int. Conf. on Wireless and Mobile Computing (WiMoB), Rome, Italy, Oct. 2017 [1]. G. Hattab and D. Cabric are with the Department of Electrical and Computer Engineering, University of California, Los Angeles, CA 90095-1594 USA (email: ghattab@ucla.edu, danijela@ee.ucla.edu).

applications. Optimization and analysis of UAV-based aggregation are studied in [24]–[27]. For example, the authors in [24] focus on optimizing the throughput of a single link between a source and a destination, assisted by a relaying UAV, whereas in our work we consider a large-scale cellular network. In [25], the authors focus on minimizing the time it takes the drone to aggregate data samples collected by IoT devices to estimate a field of interest. In [26], the authors study optimizing the UAV’s trajectory and sensors’ wake-up schedules to minimize their energy consumption. In [27], the locations and associations of the drones are optimized to minimize the transmit powers of IoT devices. Compared to the aforementioned works, we focus on optimizing the EE of IoT devices. In addition, we propose a shared spectrum access protocol between UEs and massive IoT, analyzing the impact of IoT interference on UEs.

### B. Contributions

A summary of the main contributions is given as follows.

- *Shared spectrum-based transmission protocol:* We propose a time-division duplexing (TDD) transmission protocol that provides a shared-spectrum access between massive IoT and UEs over the cellular network in the presence of UAVs that act as data aggregators for IoT devices. We use stochastic geometry [28] to characterize the average available resources for UEs and IoT devices and compare the proposed protocol with a sharing-based protocol via ACB as well as resource splitting via frequency partitioning. We also analyze the coverage performance of the UEs in the presence of IoT devices transmitting to their associated drones.
- *Energy-efficiency maximization:* We present a stochastic optimization framework that aims to optimize the transmit power of the IoT device to maximize its average EE subject to a protection criterion to its nearest UEs. For tractable analysis, the framework is given for a single-cell single-drone (SC-SD) scenario, where we derive the average EE in closed form. We further analyze the interference-to-signal ratio (ISR) at the UE in the same cell with IoT devices and use its distribution as a protection constraint. Convexity analysis is presented and the solution of the framework is discussed. Further, we discuss extensions of this framework to the case of the single-cell multi-drone (SC-MD) scenario.

We validate the theoretical expression of the EE and the optimization framework for the SC-SD and SC-MD scenarios via Monte Carlo simulations, showing that the proposed scheme provides significant EE improvements to IoT devices compared to transmitting at the maximum power, which is typically done to extend coverage [5]. The proposed scheme is further compared to ACB and orthogonal allocation in a large network. Simulations show that the EE is significantly improved for practical drone altitudes, with minimal degradation to the UE’s spectral efficiency in the UL and the DL. Such improvements are translated into an increased lifetime of IoT devices, which is validated using the 3GPP evaluation methodology in [29].

### C. Paper organization

The rest of the paper is organized as follows. The system model and the key performance metrics are presented in Section II. A comparison of the proposed transmission protocol and existing ones is presented in Section III. The EE SC-SD and SC-MD maximization frameworks are given in Section IV. Simulation results and the main conclusions are given in Section V and Section VI, respectively.

## II. SYSTEM MODEL AND PROPOSED ARCHITECTURE

### A. Cellular network model

1) *BSs and UEs:* We consider a stochastic network topology, where we model the locations of BSs using the homogeneous Poisson Point process (HPPP)  $\Phi_B$  with density  $\lambda_B$  [17]. Each BS is equipped with a multi-antenna array of size  $M_B$  and can multiplex  $U_B$  users per resource block. During downlink (DL) data communications, the BS transmits at a fixed power of  $P_B$ , such that each multiplexed user is equally allocated a power of  $P_B/U_B$ . For UEs, we assume that they are generated from an independent HPPP  $\Phi_U$  with density  $\lambda_U$ , where each one is equipped with a single-antenna system and connects to the nearest BS. During uplink (UL) data communications, the UE transmits at a fixed power of  $P_U$ .

2) *Ground-to-ground channel model:* For ground-to-ground links, e.g., BS-UE links, we assume a power-law path loss model with a loss of  $L_0$  at a reference distance of 1m and a decaying exponent of  $\alpha_G$ . For small-scale fading, we assume a Rayleigh fading channel, with gamma distributed channel power gains, as they model a variety of multi-antenna transmission modes [30]. Specifically, the channel power gains between the UE and the tagged BS and the UE and an interfering BS are, respectively, modeled as  $g_B \sim \Gamma(\Delta_B, 1)$  and  $f_B \sim \Gamma(\Psi_B, 1)$ . For instance, if the BS uses multi-user zero-forcing transmit beamforming, then  $\Delta_B = M_B - U_B + 1$  and  $\Psi_B = U_B$  [30].

We remark that we focus on a single-tier network for easier exposition in the subsequent analysis. However, it is straightforward to extend this work to multi-tier heterogeneous networks as we have done in our prior work in [1].

### B. IoT devices model

Besides providing connectivity to UEs, the cellular network must also provide connectivity to a large number of IoT devices, which are assumed to operate mainly in the UL [4]. Furthermore, we assume that IoT devices are clustered either inherently, e.g., deploying sensors in hotspots to monitor the same physical phenomenon [17], or via a clustering algorithm, as done in [27]. To this end, we model the locations of IoT devices using an independent clustered HPPP process. In particular and similar to [17], we consider the Matern cluster process, where the locations of cluster centers, i.e., parent points, is modeled by the independent HPPP  $\Phi_{CI}$  with density  $\lambda_{CI}$ . In each cluster, IoT devices represent the daughter points of the clustered process, denoted by  $\Phi_M$ , and they are uniformly distributed in a disk of radius  $R$  and with density  $\lambda_M$ . Thus, the average density of IoT devices in the network is

$\lambda_M \lambda_{CI}$ . Finally, we assume all IoT devices are single-antenna transmitters, and they transmit at a fixed power of  $P_M$ .

Applications where such IoT models are reasonable include the mass deployment of IoT devices across a city, where sensors can be anchored on bridges for infrastructure monitoring, on buildings for utility metering, or in a farm for water management [4]. Such applications are delay tolerant, yet they require reliable coverage and a very long lifetime.

### C. Proposed UAV-enabled cellular architecture

We consider deploying UAVs, e.g., drones, as a middle layer between IoT devices and the cellular infrastructure. The drone acts as a *mobile data aggregator* that is sent by a BS to provide coverage for a cluster of IoT devices. We note that while drones can be used as BSs or relays for UE traffic, as discussed in [19], in this work we primarily use them as aggregators for IoT devices that have delay-tolerant traffic. We assume the density of drones,  $\lambda_D$ , is equal to the density of clusters, i.e.,  $\lambda_D = \lambda_{CI}$ , and each one flies at an altitude of  $h_D$ . We note that fewer drones can be also used, e.g., a drone can serve multiple clusters by moving from one point to another over time. Further, the drone is equipped with an omnidirectional single-antenna cellular transceiver. We discuss the case of a multi-tier drone network, where each tier is defined by a different altitude, in Section IV-D.

1) *Initial access phase*: Since we focus on massive IoT applications with machines and sensors anchored to fixed locations, it is reasonable to assume that the locations of IoT devices in the cluster are registered in a server or a database, and hence they are known to the mobile operator [4], [27]. In particular, the drone, which is sent by the BS, moves to predetermined *stop points* for UL data aggregation. In this work and for tractable analysis, the stop point of the  $l$ -th drone,  $(x_{D,l}, y_{D,l}, h_D)$ , is the centroid of its cluster of IoT devices. We note that such location minimizes the distance to the typical IoT device, i.e., it can be shown that  $(x_{D,l}, y_{D,l}) = \arg\min_{(x,y)} \mathbb{E}_{\Phi_M}[d_{M,l}]$ , where  $d_{M,l}$  is the 3D distance between a typical IoT device and the drone. Finally, we note that the optimization of the drone's trajectory, e.g., to maximize its lifetime [31], is outside the scope of this work.

2) *Ground-to-air channel model*: We consider the following popular ground-to-air path loss model for the link between an IoT device and the  $l$ -th drone [27], [32], [33]

$$l_{M \rightarrow D}(d_{M,l}) = \mathbb{P}_{\text{LOS}}(d_{M,l}, h_D) L_0 d_{M,l}^{-\alpha_A} + (1 - \mathbb{P}_{\text{LOS}}(d_{M,l}, h_D)) L_{\text{NLOS}} L_0 d_{M,l}^{-\alpha_A}, \quad (1)$$

where  $\mathbb{P}_{\text{LOS}}(d_{M,l}, h_D)$  is the line-of-sight (LOS) probability,  $L_{\text{NLOS}}$  is the excessive path loss due to non-LOS, and  $\alpha_A$  is the ground-to-air path loss exponent. Note that, as investigated in [33], the impact of multi-path fading is negligible in such links, and thus it is ignored. The LOS probability is found using the 3GPP UMa-AV channel model, and it can be expressed as [18]

$$\mathbb{P}_{\text{LOS}}(d_{M,l}, h_D) = \min \left\{ \frac{\xi_1}{r_{M,l}}, 1 \right\} \left( 1 - e^{-r_{M,l}/\xi_2} \right) + e^{-r_{M,l}/\xi_2}, \quad (2)$$

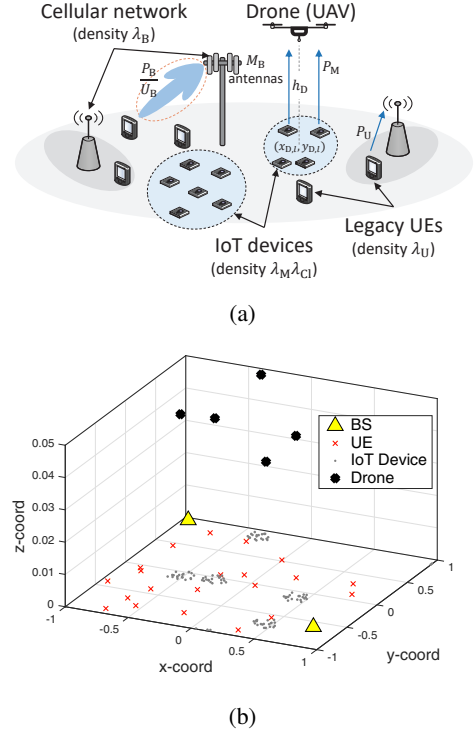


Fig. 1: (a) The proposed UAV-enabled cellular architecture; (b) A spatial realization of the network topology ( $\lambda_U = 5\lambda_B$ ,  $\lambda_D = \lambda_B$ , and  $\lambda_M = 20/\text{cluster}$ ).

where  $r_{M,l} = \sqrt{d_{M,l}^2 - h_D^2}$ , and  $\xi_1$  and  $\xi_2$  are some constants as given in [18, Table B-1]. For the link between the BS and the drone, we consider a similar model, which is expressed as

$$l_{B \rightarrow D}(d_{B,l}) = L_{\text{STR}} \cdot \left( \mathbb{P}_{\text{LOS}}(d_{B,l}, h_D) L_0 d_{B,l}^{-\alpha_A} + (1 - \mathbb{P}_{\text{LOS}}(d_{B,l}, h_D)) L_{\text{NLOS}} L_0 d_{B,l}^{-\alpha_A} \right), \quad (3)$$

where the attenuation  $L_{\text{STR}}$  is due to the fact that the BS's antenna array steering direction typically points horizontally or is tilted downwards when communicating with ground users [34]. Such attenuation depends on the drone's relative location with the array's boresight. However, we assume it to be constant for tractable analysis, which is reasonable when the drone is flying at heights higher than the BS's antenna height.

The UAV-enabled cellular network is shown in Fig. 1a, where a drone is sent by a BS to a cluster of IoT devices, stops at  $(x_{D,l}, y_{D,l})$  to collect data from IoT devices, and then aggregates the traffic to the BS. An illustration of one realization of the network is also shown in Fig. 1b. A summary of the main parameters is given in Table I.

### D. Performance Metrics

We consider two metrics: the spectral efficiency (SE) of a typical UE in the UL and DL and the energy efficiency (EE) of a typical IoT device, which are defined next.

TABLE I: Main parameters and their values if applicable

Description	Parameters	Value(s) (if applicable)
Path loss parameters	$\alpha_G$ : Path loss exponent for ground-to-ground links	$\alpha_G = 3.5$
	$\alpha_A$ : Path loss exponent for ground-to-air links	$\alpha_A = 2.2$ [18]
	$L_0$ : Path loss at a reference distance of 1m	$L_0 = -38\text{dB}$
	$L_{\text{NLOS}}$ : Additional non-LOS path loss	$L_{\text{NLOS}} = -20\text{dB}$ [32]
	$L_{\text{STR}}$ : Additional path loss due to BS's antenna array steering direction	$L_{\text{STR}} = -30\text{dB}$ [18]
BS parameters	$P_B$ : BS transmit power	$P_B = \{46, 32\}\text{dBm}$
	$M_B$ : Number of antennas at the BS	$M_B = 32$
	$U_B$ : Number of spatially multiplexed users	$U_B = 4$
UE parameters	$P_U$ : UE transmit power	$P_U = 23\text{dBm}$
	$\tau_{U,k}$ : SINR threshold	from $-5$ to $30\text{dB}$
IoT device parameters	$P_M^{\text{max}}$ : Maximum allowable transmit power	$P_M^{\text{max}} = 23\text{dBm}$
	$P_M^{\text{min}}$ : Minimum allowable transmit power	$P_M^{\text{min}} = 1\text{dBm}$
	$P_{\text{CP}}$ : Circuit power consumption	$P_{\text{CP}} = 90\text{mW}$
	$\eta$ : PA efficiency	$\eta = 0.44$ [29]
	$\tau_{M,k}$ : SINR threshold	from $-5$ to $10\text{dB}$
	$R$ : Cluster radius	$R = 50\text{m}$

1) *UE Spectral Efficiency*: We consider the UE to employ a multi-modulation and coding scheme, and thus the spectral efficiency of a typical UE in the DL/UL is defined as [35]

$$C_{U,\xi} = \bar{\beta}_{U,\xi} \sum_{k=1}^{K_U} \log_2(1 + \tau_{U,k}) \mathbf{1}(\tau_{U,k+1} \geq \gamma_{U,\xi} \geq \tau_{U,k}), \quad (4)$$

where  $\xi \in \{\text{DL}, \text{UL}\}$ ,  $\gamma_{U,\xi}$  is the signal-to-interference-plus-noise ratio (SINR),  $\{\tau_{U,k}\}$  are the SINR thresholds,  $\mathbf{1}(\cdot)$  is the indicator function, and  $\bar{\beta}_{U,\xi}$  is a pre-log term that denotes the UE long-term available resources in time, frequency, and space. This rate model assumes  $K_U$  possible thresholds, and it is a generalization of the single-rate model, i.e.,  $K_U = 1$ , that is commonly used in the literature [30], [36]. For tractable analysis, we use the mean load approximation to characterize the BS load, i.e., we assume that the load  $\bar{\beta}_{U,\xi}$  is independent of  $\gamma_{U,\xi}$  [35], [36]. We relax this assumption when we run Monte Carlo simulations.

2) *IoT Energy Efficiency*: Since the majority of IoT devices are battery-powered, the EE of the transmission protocol is critical, which is defined as the ratio of the achieved rate to the total power consumption. More formally, the EE of a typical IoT device is defined as [37]

$$E_M = \frac{\bar{\beta}_M \sum_{k=1}^{K_M} \log_2(1 + \tau_{M,k}) \mathbf{1}(\tau_{M,k+1} \geq \gamma_M \geq \tau_{M,k})}{P_{\text{CP}} + \eta^{-1} P_M}, \quad (5)$$

where  $P_{\text{CP}}$  is a constant that quantifies the circuit power consumption,  $\eta$  is the power amplifier efficiency, and  $\bar{\beta}_M$  and  $\gamma_M$  are the IoT device long-term resources and SINR, respectively. We have the following remarks about this metric. First, observe that if the device supports only a single modulation scheme, then, we can set  $K_M = 1$ . Second, the metric is also relevant to applications where coverage is paramount. For example, the value of  $\tau_{M,1}$  determines the minimum coverage needed since a zero rate, and hence zero EE, is achieved if  $\gamma_M < \tau_{M,1}$ . Last, we only focus on optimizing the link between the IoT device and the drone. The link between the drone and the BS can be

optimized separately, e.g., the drone can get closer to the BS to ensure reliable aggregation [38], the drone can compress data generated from devices performing a similar task [39], or the drone can itself be a BS [19]. Since this link is studied in the aforementioned works, it is outside the scope of this paper.

### III. PROPOSED TRANSMISSION PROTOCOL

In this section, we present the proposed transmission protocol to enable shared spectrum access between massive IoT and UEs over UAV-enabled cellular networks. We then analyze the average allocated resources of the UE and the IoT device under the proposed protocol and compare it to those achieved under existing transmission protocols.

We focus on TDD cellular networks, and thus the proposed protocol is divided into two slots:  $T_1$  and  $T_2$ . In the first time slot, the UE operates in the UL, communicating with its tagged BS. Similarly, in this slot, we treat the drone as another UE, which aggregates previously collected data from IoT devices and sends it to its tagged BS. In the second time slot, the UE operates in the DL, whereas the IoT device operates in the UL, communicating with its associated drone, as shown in Fig. 2a. The proposed protocol is motivated as follows.

- **Maximum bandwidth**: The protocol allows the IoT device to share the same time-frequency block with the UE, i.e., no resource splitting is used.
- **Reducing congestion**: When the UE operates in the UL, it competes for scheduling with drones instead of IoT devices, and thus the channel congestion is significantly reduced.
- **Limiting the impact of IoT interference**: The shared access paradigm inevitably leads to additional interference from IoT devices into UEs. However, when IoT devices transmit data in the UL, UEs operate in the DL, where their tagged BSs transmit at much higher power than the transmit power of IoT devices as  $P_B \gg P_M$ .

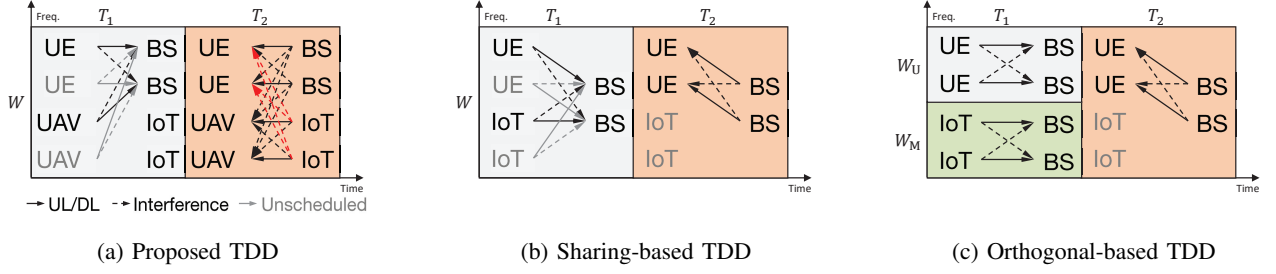


Fig. 2: Comparison of the different TDD transmission protocols.

#### A. Characterization of average resources in the proposed and existing protocols

For tractable analysis, we assume that a proportional fair scheduler is used, e.g., round-robin, and thus under the mean load approximation [36], the average load is inversely proportional to the average number of devices connected to the same source.

1) *Proposed protocol*: Let  $\bar{\beta}_{U,UL}^P$  denote the average allocated resources to a typical UE operating in the UL under the proposed protocol. Then, it can be shown that

$$\begin{aligned} \bar{\beta}_{U,UL}^P &\stackrel{(a)}{=} \underbrace{W}_{\text{Freq.}} \times \underbrace{U_B}_{\text{Space}} \times \underbrace{T_1 \left( \frac{1}{N_{B,UL}^P} \right)}_{\text{Time}} \\ &\stackrel{(b)}{=} W \times U_B \times T_1 \left( \frac{\lambda_B}{\lambda_U + \lambda_D} \right), \end{aligned} \quad (6)$$

where (a) follows since the entire bandwidth  $W$  is allocated to the UE,  $U_B$  UEs can be spatially multiplexed by the same BS, and the portion of the time allocated to the UE is inversely proportional to the average number of devices connected to the BS, i.e.,  $N_{B,UL}^P$ . Here, (b) follows by showing that the average number of UEs (or drones) connected to the BS under the nearest BS association is  $\lambda_U/\lambda_B$  (or  $\lambda_D/\lambda_B$ ) [36]. Similarly, the average portion of resources of the UE in the DL is expressed as  $\bar{\beta}_{U,DL}^P = W \times U_B \times T_2 \left( \frac{\lambda_B}{\lambda_U} \right)$ , which follows since in the second time slot, no IoT devices are connected to the BS under the proposed protocol. For the IoT device, it can be shown that the average portion of resources is given as  $\bar{\beta}_M^P = W \times T_2 \lambda_M^{-1}$ , which follows since the average number of IoT devices per cluster is  $\lambda_M$ , and the drone multiplexes one IoT device per time-frequency slot. Note that for low-rate applications, the drone can divide the bandwidth  $W$  into smaller frequency blocks and serve multiple IoT devices, one per frequency block. This does not change  $\bar{\beta}_M^P$  since the decrease in frequency resources is equally compensated by increased time resources.

2) *Comparison with sharing-based protocol*: In the sharing-based protocol, the IoT device is registered as another UE, as shown in Fig. 2b. To control channel congestion, the 3GPP standard proposes one mechanism, namely *access class barring* (ACB), which prioritizes UE traffic over IoT devices [7]. More formally, each BS broadcasts a parameter  $0 \leq \kappa \leq 1$  to all IoT devices in vicinity. The IoT device then generates a random number  $n \in [0, 1]$  before initiating a channel access request. If  $n > \kappa$ , then the IoT device does not request access.

Clearly, for  $\kappa = 1$ , the protocol simplifies to a standard sharing protocol that is agnostic to the device type. Let  $\bar{\beta}_{U,UL}^S$  denote the average allocated resources to a typical UE operating in the UL under the sharing-based protocol. Then, we have  $\bar{\beta}_{U,UL}^S = W \times U_B \times T_1 \left( \frac{\lambda_B}{\lambda_U + \kappa \lambda_M \lambda_{CI}} \right)$ , which follows since the average number of IoT devices per BS is  $\lambda_M \lambda_{CI} / \lambda_B$ , yet only a fraction,  $\kappa$ , of them request access. Clearly, for  $\bar{\beta}_{U,UL}^S > \bar{\beta}_{U,UL}^P$ , we must have  $\kappa < \lambda_M^{-1}$ , yet this degrades the average resources allocated to the IoT device. Indeed, the average allocated resource of a typical IoT device under the sharing protocol is given as

$$\begin{aligned} \bar{\beta}_M^S &= \mathbb{P}(n > \kappa) \bar{\beta}_{M|n>\kappa}^S + \mathbb{P}(n \leq \kappa) \bar{\beta}_{M|n \leq \kappa}^S \\ &= W \times U_B \times \kappa T_1 \left( \frac{\lambda_B}{\lambda_U + \kappa \lambda_M \lambda_{CI}} \right) \\ &\stackrel{(a)}{\leq} \bar{\beta}_M^P \left( \frac{U_B \lambda_B}{\lambda_U + \lambda_{CI}} \right), \end{aligned} \quad (7)$$

where (a) follows using  $\kappa < \lambda_M^{-1}$  and assuming  $T_1 = T_2$ . Since the density of UEs is typically higher than the density of BSs, i.e.,  $\lambda_U \gg U_B \lambda_B$ , we get  $\bar{\beta}_M^S < \bar{\beta}_M^P$ . Finally, for the second time slot, we have  $\bar{\beta}_{U,DL}^S = \bar{\beta}_{U,DL}^P$  for the UE.

3) *Comparison with orthogonal-based protocol*: Alternative to using ACB to resolve channel congestion, 3GPP has also proposed the separation of frequency resources [7], as shown in Fig. 2c. Let  $W_U \in [0, W]$  be the portion of the spectrum allocated for UEs, then the average portion of allocated resources for a typical UE in the UL under this protocol is  $\bar{\beta}_{U,UL}^O = W_U \times U_B \times T_1 \left( \frac{\lambda_B}{\lambda_U} \right)$ . If  $W_U/W > \lambda_U/(\lambda_U + \lambda_D)$ , then we have  $\bar{\beta}_{U,UL}^O > \bar{\beta}_{U,UL}^P$ . However, this comes at the expense of reducing the resources allocated to the IoT device since we have

$$\begin{aligned} \bar{\beta}_M^O &= W_M \times U_B \times T_1 \left( \frac{\lambda_B}{\lambda_M \lambda_{CI}} \right) \\ &\stackrel{(a)}{<} W \times U_B \times \frac{T_1}{\lambda_M} \left( \frac{\lambda_B}{\lambda_U + \lambda_{CI}} \right) \\ &\stackrel{(b)}{<} \bar{\beta}_M^P, \end{aligned} \quad (8)$$

where (a) follows from the fact that  $W_M = W - W_U$  and thus  $\frac{W_U}{W} > \frac{\lambda_U}{\lambda_U + \lambda_{CI}} \iff \frac{W_M}{W} < \frac{\lambda_{CI}}{\lambda_U + \lambda_{CI}}$ . In addition, (b) follows assuming  $T_1 = T_2$  and the density of UEs is high. Finally and similar to the sharing-based protocol, we have  $\bar{\beta}_{U,DL}^O = \bar{\beta}_{U,DL}^P$  for the UE.

To summarize, for the sharing protocol to outperform the proposed one in terms of resource allocation for the UE,

we must use aggressive ACB with very small values of  $\kappa$ , which inevitably affects the IoT EE as the average portion of allocated resources is decreased. For the orthogonal allocation to outperform the proposed protocol in terms of the UE performance, nearly all resources should be allocated to the UE, i.e.,  $W_U \rightarrow W$ , since  $\lambda_U \gg \lambda_D$ , and this also limits the resources allocated to the IoT device.

### B. Analysis of IoT Interference on UEs

While the proposed protocol improves the average allocated resources of a typical UE, in comparison with sharing-based and orthogonal-based protocols, the signal-to-interference ratio (SIR) of a typical UE degrades due to the presence of an additional interference term generated from IoT devices (cf. Fig. 2a). Specifically, the SIR of a typical UE can be written as

$$\tilde{\gamma}_{U,DL}^P = \frac{\frac{P_B}{U_B} g_B L_0 x_B^{-\alpha_G}}{\sum_{y_b \in \Phi'_B} \frac{P_B}{U_B} f_b L_0 y_b^{-\alpha_G} + \sum_{z_m \in \Phi'_M} P_M f_m L_0 z_m^{-\alpha_G}}, \quad (9)$$

where  $\Phi'_B$  is the set of interfering BSs,  $\Phi'_M$  is the set of interfering IoT devices,  $f_m \sim \Gamma(1, 1)$ ,  $x_B$  is the distance to the tagged BS,  $y_b$  is the distance to the  $b$ -th interfering BS, and  $z_m$  is the distance to the  $m$ -th interfering IoT device. Next, we derive the coverage probability of the UE under the proposed protocol to highlight the key parameters that affect the UE's coverage.

The coverage probability is defined as  $\mathbb{C}_{U,DL}^P(\tau) \triangleq \mathbb{P}(\tilde{\gamma}_{U,DL}^P \geq \tau)$ , which can be rewritten as

$$\mathbb{C}_{U,DL}^P(\tau) \stackrel{(a)}{=} 2\pi\lambda_B \int_0^\infty x \mathbb{E}_{g_B} \left[ F_{I_U} \left( \frac{g_B}{\tau x^{\alpha_G}} \right) \right] e^{-\pi\lambda_B x^2} dx, \quad (10)$$

where (a) follows from the distribution of the distance from the UE to the tagged BS [36] and  $F_{I_U}(\cdot)$  is the cumulative distribution function (CDF) of the interference. Using the Gil-Pelaez Inversion theorem [40] to compute the interference CDF, we get the following theorem.

**Theorem 1.** *The coverage probability of the UE under the proposed protocol is expressed as*

$$\mathbb{C}_{U,DL}^P(\tau) = \frac{1}{2} - \frac{\Upsilon(\tau, \lambda_B, \lambda_D, \hat{P}_{B,M})}{\pi}, \quad (11)$$

where  $\hat{P}_{B,M} = \text{sinc}^{-1}(\delta_G) P_M U_B / P_B$ ,  $\delta_G = 2/\alpha_G$ , and

$$\Upsilon(\tau, \lambda_B, \lambda_D, \hat{P}_{B,M}) = \int_0^\infty \frac{1}{t} \text{Im} \left\{ \frac{(1+jt/\tau)^{-\Delta_B}}{{}_2F_1(\delta_G, \Psi_B; 1-\delta_G; jt) + \frac{\lambda_D}{\lambda_B} \hat{P}_{B,M}^{\delta_G} (-jt)^{\delta_G}} \right\} dt. \quad (12)$$

*Proof:* See Appendix A. ■

The expression is given in a single integral form that can be efficiently evaluated using numerical software. The key insight here is that the degradation of the UE coverage due to the presence of IoT devices depends mainly on two factors: (i) the ratio of the transmit power of the IoT device to the power allocated to the UE, i.e.,  $P_M/(P_B/U_B)$  and (ii) the average number of drones per BS, i.e.,  $\lambda_D/\lambda_B$ . To see this, note that the coverage probability in the absence of IoT devices is  $\mathbb{C}_{U,DL}^N(\tau) = \frac{1}{2} - \frac{1}{\pi} \int_0^\infty \frac{1}{t} \text{Im} \left\{ \frac{(1+jt/\tau)^{-\Delta_B}}{{}_2F_1(\delta_G, \Psi_B; 1-\delta_G; jt)} \right\} dt$ , and

thus using stochastic dominance, i.e.,  $\mathbb{C}_{U,DL}^N(\tau) \geq \mathbb{C}_{U,DL}^P(\tau)$ , we have

$$\int_0^\infty \frac{\text{Im} \left\{ \frac{(1+jt/\tau)^{-\Delta_B}}{{}_2F_1(\delta_G, \Psi_B; 1-\delta_G; jt)} \right\}}{t} dt \leq \Upsilon(\tau, \lambda_B, \lambda_D, \hat{P}_{B,M}), \quad (13)$$

where the gap above decreases as  $\lambda_D/\lambda_B \rightarrow 0$  and/or  $P_M/(P_B/U_B) \rightarrow 0$ .

We validate the theoretical expression with Monte Carlo simulations, using the same parameters in Table I. Fig. 3a shows the distribution of coverage in the presence and absence of IoT devices. It is observed that increasing the number of drones decreases the coverage, yet the degradation is not severe, e.g., the median SIR merely degrades by 1.7dB under the proposed protocol with  $\lambda_D/\lambda_B = 5$ . Recall that here a drone is assigned to a single cluster. However, if a single drone is assigned instead to serve multiple clusters, moving from one stop point to another, then the interference on UEs from IoT transmission decreases, e.g., median SIR degradation is less than 0.36dB when  $\lambda_D/\lambda_B = 1$ . Nevertheless, the cost of reducing this interference is the increased delay on IoT devices, leading eventually to degradation of the IoT energy efficiency when  $\lambda_M \lambda_{Cl} \gg 1$ . To this end, another approach to limit the interference is to reduce the IoT transmit power, as shown in Fig. 3b. In the next section, we focus on optimizing the IoT transmit power such that the IoT EE is maximized and the IoT interference is controlled.

## IV. IOT ENERGY-EFFICIENCY MAXIMIZATION

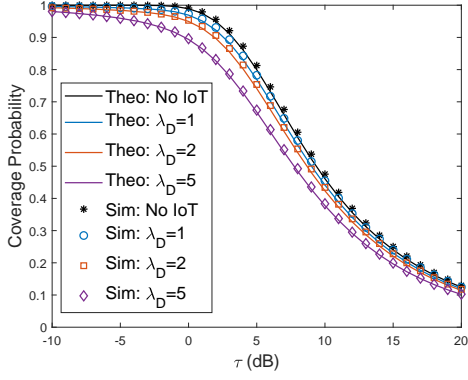
In this section, we present a stochastic optimization framework that maximizes the average EE of an IoT device under the proposed protocol. The framework takes the following form

$$\begin{aligned} & \underset{P_M}{\text{maximize}} && \mathbb{E}[E_M] \\ & \text{subject to} && f(I_U) \leq \epsilon, \\ & && P_M \in \mathcal{P}, \end{aligned} \quad (14)$$

where the  $f(\cdot)$  is an interference constraint to protect UEs and  $\mathcal{P}$  is the feasible set of transmit powers. We have the following remarks about the problem in (14). First, it is a stochastic optimization framework, as the objective function is the mean of a random variable, and the expectation is taken with respect to spatial realizations. Second, such formulation aims to optimize a single variable  $P_M$ , significantly reducing the complexity of implementation, i.e., once the problem is solved, the network or the drone broadcasts the optimal transmit power, over a control channel<sup>1</sup>, to all of its IoT devices. Thus, all devices belonging to the same cluster use the same transmit power, which maximizes on *average* the EE, i.e., this approach does not necessarily maximize the EE of every device as a single value is used, yet it significantly reduces the control overhead. Third, the constraint is a function of the interference from IoT devices into UEs. We do not enforce a UE rate

<sup>1</sup>In LTE and 5G-NR, the BS sends power control commands via the downlink control information (DCI) over the physical downlink control channel (PDCCH). Once the device successfully decodes the DCI, it follows the power control commands on the uplink channel.





(a) Variations of SIR threshold

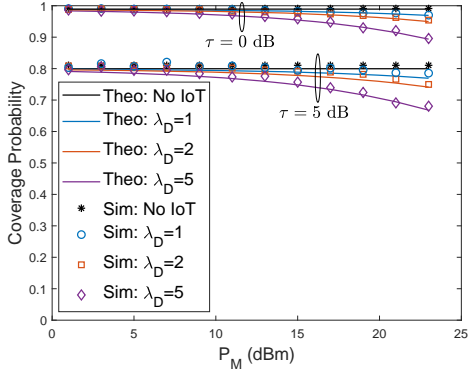
(b) Variations of IoT transmit power,  $P_M$ 

Fig. 3: The UE DL coverage performance with and without IoT devices.

constraint because this would incur additional overhead due to the necessary coordination between UEs and UAVs.

There are two challenges to solve (14). The first one is that the objective function is intractable due to the ground-to-air channel model from interfering BSs and IoT devices into drones. The second one is that the UE coverage probability in (11) is given in an integral form, making it not amenable to use as a UE protection criterion. For these reasons, we focus on optimizing the EE in a single-cell single-drone (SC-SD) setting, i.e., we ignore the interference from BSs and IoT devices outside the cell of the typical IoT device. Such framework is shown to be tractable, which helps glean useful insights. We will further evaluate the solution of the SC-SD framework in the large network case, i.e., many drones and many cells, via Monte Carlo simulations.

#### A. Average IoT EE in the SC-SD Case

Let  $\hat{E}_M$  and  $\hat{\gamma}_M$  denote the IoT EE and IoT UL SINR in the SC-SD case, respectively, and let  $p = P_M$  for notational simplicity. Then, the average EE under the proposed protocol, i.e.,  $\bar{E}_M(p) \triangleq \mathbb{E}[\hat{E}_M]$ , can be written as

$$\bar{E}_M(p) = \frac{\bar{\beta}_M^P \sum_{k=1}^{K_M} \mu_k \mathbb{P}(\hat{\gamma}_M(p) \geq \tau_{M,k})}{P_{CP} + \eta^{-1}p}, \quad (15)$$

where  $\mu_1 = \log_2(1 + \tau_{M,1})$  and  $\mu_k = \log_2(1 + \tau_{M,k+1}) - \log_2(1 + \tau_{M,k})$  for  $k > 1$ .

In a single cell, the drone receives signals from IoT devices in its cluster and receives interference from the tagged BS, which operates in the DL. The next proposition presents the distributions of the received desired signal and interference powers at the drone, which will be useful to evaluate  $\mathbb{P}(\hat{\gamma}_M(p) \geq \tau_{M,k})$ .

**Proposition 1.** *The distribution of the desired signal power,  $S_M = P_M L_{M \rightarrow D}(d_{M,l})$ , at a typical drone is expressed as*

$$\mathbb{P}(S_M \leq \tau) = 1 - \frac{(P_M L_M / \tau)^{\delta_A} - h_D^2}{R^2}, \quad (16)$$

where  $\delta_A = 2/\alpha_A$ ,  $L_M = L_0((1 - L_{NLOS})\bar{\mathbb{P}}_{LOS,M} + L_{NLOS})$ ,  $\bar{\mathbb{P}}_{LOS,M}$  is the average of (2), which is computed numerically, and  $\tau \in [P_M L_M (R^2 + h_D^2)^{-1/\delta_A}, P_M L_M h_D^{-\alpha_A}]$ . In addition, the distribution of the interference signal power  $I_B = P_B L_{B \rightarrow D}(d_{B,l})$  is given as

$$\mathbb{P}(I_B \leq \tau) = \exp(\pi \lambda_B h_D^2) \cdot \exp(-\pi \lambda_B (P_B L_B / \tau)^{\delta_A}), \quad (17)$$

where  $L_B = L_0((1 - L_{NLOS} L_{STR})\bar{\mathbb{P}}_{LOS,B} + L_{NLOS} L_{STR})$  and  $\tau \in [0, P_B L_B h_D^{-\alpha_A}]$ .

*Proof:* See Appendix B. ■

*Remark:* It is observed from (16) that as  $h_D$  increases, the variations in  $S_M$  reduces since  $\tau \in [P_M L_M (R^2 + h_D^2)^{-1/\delta_A}, P_M L_M h_D^{-\alpha_A}]$ , i.e., the distribution of  $S_M$  becomes more concentrated around the median. This follows because the drone location is optimized to reduce the average 2D distance to a typical IoT device, increasing the LOS probability particularly when  $h_D \geq R$ . Similarly, it is observed from (17) that increasing the density of BSs increases the interference as the average distance between the drone and its tagged BS decreases. Furthermore, it can be shown that increasing the drone's height decreases  $I_B$ , but not as rapidly as the decrease in  $S_M$ .

Using Proposition 1, we derive the coverage probability and the average EE of the IoT device.

**Theorem 2.** *The coverage probability of an IoT device in the SC-SD case is given as*

$$\mathbb{P}(\hat{\gamma}_M \geq \tau) \approx e^{\pi \lambda_B h_D^2} \cdot \exp\left(-\pi \lambda_B \left(\frac{P_M \tilde{L}_M}{P_B L_B} - \frac{P_N}{\tau}\right)^{-\delta_A}\right), \quad (18)$$

where  $\tilde{L}_M = L_M (R^2 + h_D^2)^{-1/\delta_A}$  and  $P_N$  is the noise power. In addition, the average EE of an IoT device is expressed as

$$\bar{E}_M(p) = \frac{\bar{\beta}_M^P e^{\pi \lambda_B h_D^2} \sum_{k=1}^{K_M} \mu_k e^{-\frac{\pi \lambda_B}{(P_B L_B)^{-\delta_A}} \left(\frac{p \tilde{L}_M}{\tau_k} - P_N\right)^{-\delta_A}}}{P_{CP} + \eta^{-1}p}. \quad (19)$$

*Proof:* The coverage probability can be written as

$$\mathbb{P}(\hat{\gamma}_M \geq \tau) \triangleq \mathbb{P}\left(\frac{S_M}{I_B + P_N} \geq \tau\right) \approx \mathbb{P}\left(I_B \leq \frac{\tilde{S}_M}{\tau} - P_N\right), \quad (20)$$

where we have used the median received signal power  $\tilde{S}_M$  computed from (16) to approximate the coverage (recall that  $S_M$  has small variations particularly when  $h_D \geq R$ ). Thus, using (17), we arrive at (18). ■

### B. IoT Interference Constraint

In this section, we propose to use the distribution of the interference-to-signal ratio (ISR) as a protection criterion. We note that in [41], the mean of ISR (MISR) has been used as a metric to compare different interference mitigation techniques over cellular networks with stochastic topologies. Yet, using the ISR distribution provides more flexibility compared to the MISR, e.g., the protection criterion can be designed to limit the median, the 95th percentile, etc. The ISR is defined as  $\text{ISR}_U = \frac{\mathbb{E}_{f_M}[\hat{I}_{U,M}]}{\mathbb{E}_{g_B}[S_B]}$ , where  $\hat{I}_{U,M}$  is the interference from the typical IoT device to its nearest UE and  $S_B$  is the received desired signal power at the UE from its tagged BS. We note, similar to the MISR metric, the expectation is first taken with respect to channel realizations. The distribution is thus given as

$$\begin{aligned} \mathbb{P}(\text{ISR}_U \geq \rho) &\stackrel{(a)}{=} \mathbb{P}\left(\frac{P_M z_M^{-\alpha_G}}{\frac{\Delta_B P_B}{U_B} z_B^{-\alpha_G}} \geq \rho\right) \\ &= \mathbb{P}\left(\frac{z_B}{z_M} \geq \left(\rho \frac{\Delta_B P_B}{U_B P_M}\right)^{1/\alpha_G}\right) \\ &\stackrel{(b)}{=} \mathbb{E}_{z_M} \left[ \exp\left(-\pi \lambda_B z_M^2 \left(\rho \frac{\Delta_B P_B}{U_B P_M}\right)^{\delta_G}\right) \right] \\ &\stackrel{(c)}{=} \left[ 1 + \frac{\lambda_B}{\lambda_U} \left(\rho \frac{\Delta_B P_B}{U_B P_M}\right)^{\delta_G} \right]^{-1}, \end{aligned} \quad (21)$$

where (a) follows from the mean of desired and interference power channel gains, (b) follows using the complementary CDF of the distance from the UE to its tagged BS, and (c) follows by taking the expectation with respect to the distance between the IoT device and the nearest UE.

### C. SC-SD Stochastic Optimization Framework

Using (19) as an objective function and the ISR expression in (21) as an interference constraint, i.e.,  $f(I_U) \leq \epsilon \Leftrightarrow \mathbb{P}(\text{ISR}_U \geq \rho) \leq \epsilon$ , we get the following optimization problem

$$\begin{aligned} &\underset{P_M}{\text{maximize}} && \frac{\sum_{k=1}^{K_M} \mu_k \exp\left(-\frac{\pi \lambda_B}{(P_B L_B)^{-\delta_A}} \left(\frac{P_M \tilde{L}_M}{\tau_k} - P_N\right)^{-\delta_A}\right)}{P_{CP} + \eta^{-1} P_M} \\ &\text{subject to} && P_M \leq \rho \left(\frac{\Delta_B P_B}{U_B}\right) \left(\frac{\lambda_B}{\lambda_U} \cdot \frac{\epsilon}{1-\epsilon}\right)^{1/\delta_G}, \\ &&& P_M^{\min} \leq P_M \leq P_M^{\max}, \end{aligned} \quad (22)$$

where  $P_M^{\min}$  and  $P_M^{\max}$  are the minimum and maximum allowable transmit powers, respectively. In what follows, we denote the numerator of the objective function, i.e., the rate, by  $r(P_M)$ , and the denominator, i.e., power consumption, by  $c(P_M)$ . The following proposition shows that the problem in (22) is quasiconcave, and thus a local maximum is a global one [42].

**Proposition 2.** *The objective function in (22) is quasiconcave and unimodal, whereas the constraints are all affine. Hence, the optimization problem is quasiconcave.*

*Proof:* The proof follows from showing that  $r(p)$  is S-shaped in  $p$  (see Appendix C). ■

### Algorithm 1 Dinkelbach's algorithm to solve the SC-SD optimization

---

```

1: procedure ( $\zeta > 0; i = 0; \nu_i = 0$ )
2:   while  $H(\nu_i) > \zeta$  do
3:     Compute  $\Gamma = \text{ROOT}(r'(p) - \eta^{-1} \nu_i)$ 
4:      $p_i^* = \min \left\{ P_M^{\max}, \rho \left( \frac{\Delta_B P_B}{U_B} \right) \left( \frac{\lambda_B}{\lambda_U} \cdot \frac{\epsilon}{1-\epsilon} \right)^{1/\delta_G}, \Gamma \right\}$ 
5:      $H(\nu_i) = r(p_i^*) - \nu_i c(p_i^*)$  and  $\nu_{i+1} = \frac{r(p_i^*)}{c(p_i^*)}$ 
6:      $i = i + 1$ 
7:   end while
8:   return  $P_M^* = p_i^*$ 
9: end procedure

```

---

Since the problem has a single optimizing variable, a line search is sufficient to solve the problem. However, in what follows we discuss a specific algorithm to solve the problem, as its generalization will be used for the SC-MD case in Section IV-D. To solve the optimization problem, we note that if the following condition is satisfied

$$\tau_k \leq \frac{P_M^{\min} \tilde{L}_M}{P_N + P_B L_B \left( \frac{\delta_A \pi \lambda_B}{1 + \delta_A} \right)^{1/\delta_A}} \quad \forall k, \quad (23)$$

then the optimization problem can be transformed from a quasiconcave problem into a concave one using the Charnes-Cooper Transform [42]. Thus, a standard convex optimization solver can be used to solve the problem. When the condition in (23) is not satisfied, i.e., for general thresholds, then the problem can be efficiently solved using the Dinkelbach's algorithm [43], which converges super-linearly to the global optimal solution. The algorithm that specifically solves (22) is summarized in Alg. 1. In essence, the algorithm seeks to find the root of the auxiliary function  $H(\nu) = \max_{p \in \mathcal{P}} \{r(p) - \nu c(p)\}$ , which is achieved at the point that maximizes the optimization problem [43]. Finally, a closed-form solution can be derived for the special case  $K_M = 1$  and  $\alpha_A = 2$ . Specifically, the objective function, in this case, is maximized at

$$\begin{aligned} p_{\text{unconst}}^* &= \frac{\tau_{M,1} (P_N + \pi \lambda_B P_B L_B)}{\tilde{L}_M} \\ &+ \frac{\sqrt{\pi \tau_{M,1} \lambda_B P_B L_B (P_N \tau_{M,1} + \tilde{L}_M \eta P_{CP})}}{\tilde{L}_M}, \end{aligned} \quad (24)$$

and thus the optimal transmit power is  $P_M^* = \min\{P_M^{\max}, \rho \left(\frac{\Delta_B P_B}{U_B}\right) \left(\frac{\lambda_B}{\lambda_U} \cdot \frac{\epsilon}{1-\epsilon}\right)^{1/\delta_G}, p_{\text{unconst}}^*\}$ . It is observed from (24) that the optimal power increases for: (i) higher target threshold  $\tau_{M,1}$  to meet the new coverage requirement, (ii) higher BS transmit power  $P_B$  or higher BS density  $\lambda_B$  to combat the increased interference from the cellular network, or (iii) higher PA efficiency  $\eta$  to utilize the decrease in power consumption.

### D. EE Optimization in heterogeneous single-cell multi-drone case

In this section, we consider the single-cell multi-drone case (SC-MD), where each cell has multiple drones, each serving a cluster of IoT devices. We can further assume each drone



belongs to a different tier, i.e., we consider an  $N$ -tier drone network such that the  $l$ -th tier drone flies at an altitude of  $h_{D,l}$  and serves an IoT cluster of radius  $R_l$ . The IoT device in a cluster served by the  $l$ -th drone transmits at power  $P_{M,l}$ .

The challenge in the multi-drone is that the objective function can no longer be given in a closed-form expression due to the complicated ground-to-air path loss model between multiple interferers and the drone. Here, the interferers, with respect to a given drone, are the tagged BS and the other IoT devices transmitting to their respective drones in the same cell. To this end, we propose to model the different interference sources in the cell as one Poissonian source with a transmit power equal to the sum of transmit powers of all interferers. Such an approach ensures a tractable formulation and will be validated in the simulations section. Under this modeling assumption, the EE of an IoT device served by the  $l$ -th drone tier can be written as

$$\bar{E}_l(\mathbf{P}_M) \triangleq \frac{\bar{\beta}_M^P e^{\pi \lambda_B h_D^2} \sum_{k=1}^{K_M} \mu_k e^{-\frac{\pi \lambda_B \left( \frac{P_{M,l} \bar{L}_{M,l} - P_N}{\tau_k} \right)^{-\delta_A}}}{P_{CP} + \eta^{-1} P_{M,l}}, \quad (25)$$

where  $\mathbf{P}_M$  is the vector of transmit powers. Next, we discuss two common formulations for the EE optimization in the SC-MD case.

1) *Max-min formulation*: In this formulation, the objective is to maximize the minimum EE of a typical IoT device. Such formulation is a conservative one that aims to improve the worst case scenario. In particular, the max-min EE maximization is given as

$$\begin{aligned} & \underset{\mathbf{P}_M}{\text{maximize}} \quad \min_l \quad \bar{E}_l(\mathbf{P}_M) \\ & \text{subject to} \quad \sum_l P_{M,l} \leq \rho \left( \frac{\Delta_B P_B}{U_B} \right) \left( \frac{\lambda_B}{\lambda_U} \cdot \frac{\epsilon}{1-\epsilon} \right)^{1/\delta_G}, \\ & \quad P_M^{\min} \leq P_{M,l} \leq P_M^{\max} \quad \forall l. \end{aligned} \quad (26)$$

The EE expression in (26) is still quasiconcave, and since the objective function is the minimum of quasiconcave functions, it remains quasiconcave. Thus, the max-min framework is quasiconcave, and can be solved using a Dinkelbach's-like algorithm.

2) *Sum-EE formulation*: In this formulation, the total EE of IoT devices in the cell is used as an objective function, and thus such formulation tends to favor IoT devices with better coverage. More formally, we have

$$\underset{\mathbf{P}_M}{\text{maximize}} \quad \sum_{l=1}^N \bar{E}_l(\mathbf{P}_M), \quad (27)$$

subject to the same constraints as in (26).

The generalized Dinkelbach's algorithm for both SC-MD formulations is given in Alg. 2, where the implementation of Sum-EE is given in brackets. We note for max-min, the algorithm converges linearly to the global optimal solution [43]. However, for the total EE formulation, the objective function is not necessarily quasiconcave, as the sum of quasiconcave functions does not preserve quasiconcavity. To this end, solving this problem globally, with limited complexity, remains an open problem, i.e., although Alg. 2 has become

---

**Algorithm 2** Generalized Dinkelbach's algorithm to solve the SC-MD optimization

---

```

1: procedure ( $\zeta > 0; i = 0; \nu_i = 0$ )
2:   while  $H(\nu) > \zeta$  do
3:      $\mathbf{P}_{M,i}^* = \underset{\mathbf{p} \in \mathcal{P}}{\text{argmax}} \left\{ \min_l \{r_l(\mathbf{p}) - \nu_i c_l(\mathbf{p})\} \right\}$ 
4:      $\left[ \mathbf{P}_{M,i}^* = \underset{\mathbf{p} \in \mathcal{P}}{\text{argmax}} \left\{ \sum_l r_l(\mathbf{p}) - \nu_i c_l(\mathbf{p}) \right\} \right]$ 
5:      $H(\nu_i) = \min_l \{r_l(\mathbf{P}_{M,i}^*) - \nu_i c_l(\mathbf{P}_{M,i}^*)\}$ 
6:      $\left[ H(\{\nu_{i,l}\}) = \sum_l r_l(\mathbf{P}_{M,i}^*) - \nu_{i,l} c_l(\mathbf{P}_{M,i}^*) \right]$ 
7:      $\nu_{i+1} = \min_l \frac{r_l(\mathbf{P}_{M,i}^*)}{c_l(\mathbf{P}_{M,i}^*)} \quad \left[ \nu_{i+1,l} = \frac{r_l(\mathbf{P}_{M,i}^*)}{c_l(\mathbf{P}_{M,i}^*)} \right]$ 
8:      $i = i + 1$ 
9:   end while
10:  return  $\mathbf{P}_M^* = \mathbf{P}_{M,i}^*$ 
11: end procedure

```

---

popular to solve sum of ratios, it does not necessarily arrive at the global optimal solution, if it exists [44].

### E. Implementation

In the single-drone case, solving Alg. 1 requires finding the roots of a sequence of auxiliary functions, which can be done by the BS. The algorithm requires prior knowledge about the BS transmission mode to determine  $\Delta_B$  and  $U_B$  as well as the network load to determine  $\lambda_B$  and  $\lambda_U$ , all are easily accessible at the BS. Since IoT devices may have varying PA efficiencies, a nominal value maybe used for a given modulation and coding scheme (MCS) to estimate the total power consumption, i.e.,  $c(p)$ . Estimating the rate, i.e.,  $r(p)$ , is easier as cellular networks already rely on rate-based metrics for link adaptation, and thus existing methods can be applied.

Since the complexity of Alg. 1 is low, the drone itself can solve the problem, yet the BS must relay the relevant information to the drone. For the multi-drone case, it is more economical to solve the Alg. 2 at the BS, eliminating the need for the drones to communicate with each other. We finally note that the solutions of the proposed algorithms can be used as nominal transmit powers, where transmit power control is further applied by each device depending on the feedback from the network.

## V. SIMULATION RESULTS

In this section, we first validate the theoretical analysis and the stochastic optimization frameworks, focusing on SC-SD and SC-MD scenarios. Then, we consider larger networks, where we compare the proposed protocol with sharing-based and orthogonal-based protocols.

Unless otherwise stated, we use the simulation parameters given in Table I. In each spatial realization of the network, we generate BSs, UEs, and IoT devices according to their distributions. Each drone then moves to their predetermined stop points. We then generate the channel power gains according to their distributions and compute the large-scale fading for all links to compute their SINR, where a thermal noise power, with spectral density  $-174\text{dBm/Hz}$ , is considered at

all receivers. Then the SE of UEs is computed via (4) and the EE IoT devices is computed via (5) for the different transmission protocols. We note that we use the actual load and LOS probability, instead of their mean, to compute the performance metrics.

#### A. Validation of the stochastic optimization frameworks

In this section, we focus on a single cell to validate the theoretical analysis. We further compare the EE performance of the SC-SD and SC-MD optimization frameworks with a scheme where the IoT device transmits at maximum power, i.e.,  $P_M = 23\text{dBm}$  [5].

1) *Impact of IoT transmit power on the EE*: We consider two IoT categories: CAT-0 and NB-IoT. In the former, the IoT device shares the entire band with the UE, i.e.,  $W = 20\text{MHz}$  and  $P_B = 46\text{dBm}$ . In the latter, the IoT only shares a single resource block, i.e.,  $W = 180\text{KHz}$  and  $P_B = 32\text{dBm}$ . For interference protection, we assume  $\epsilon = 0.5$  and  $\rho_{\text{dB}} = -6\text{dB}$ , i.e., the median ISR should not exceed  $-6\text{dB}$ . The performance of EE under different transmit powers is shown in Fig. 4a and Fig. 4b for CAT-0 and NB-IoT, respectively. It is shown that the theoretical expression in (19) matches well with Monte Carlo simulations. Further, the EE is significantly improved using the proposed SC-SD framework compared to the max-power scheme, e.g., the EE in CAT-0 of the proposed SC-SD framework is 4.5x and 3.3x that of max-power for  $h_D = 50\text{m}$  and  $h_D = 120\text{m}$ , respectively. This follows because the drone's location is optimized to minimize the 2D distance to the IoT device, requiring low transmit power for reliable coverage. Third, increasing the drone's height has two effects: an increase in the optimal transmit power and a decrease in the EE. These follow because as  $h_D$  increases, the received signal power decreases more rapidly than interference, degrading the coverage. Thus, the IoT device must transmit at higher power to combat the degradation, decreasing its EE. Finally, the NB-IoT operation is more efficient than CAT-0 since in the former the IoT device shares a smaller number of carriers with the UE, reducing the interference. In Fig. 4c, we validate the coverage approximation in (18), which is shown to be in good agreement with Monte Carlo simulations. It is also evident here that using drones at lower altitudes is critical to provide high coverage.

2) *Validation of the SC-MD case*: Next, we study the EE performance in the presence of multiple drones in the same cell. We consider each drone to fly at one of the following altitudes:  $h_D = [50, 100, 150, 200, 250]\text{m}$ . In Fig. 5a, we show the total and the minimum EE of scheduled IoT devices per cell. We compare the max-power scheme to *Max-min* and *Sum-EE* schemes, where power allocation is done using Algorithm 2. We note that the EE is computed via Monte Carlo simulations. As expected, the *Sum-EE* formulation achieves the highest total EE in a cell, yet the *Max-min* formulation provides tangible improvements to the worst case scenario, e.g., the minimum EE is 2.4x and 2.0x the minimum EE under *Max-power* and *Sum-EE*, respectively. We further show the EE of IoT devices that belong to the different drones in Fig. 5b. It is observed that the *Max-min* solution aims to improve the EE of devices connected to the drone with the highest

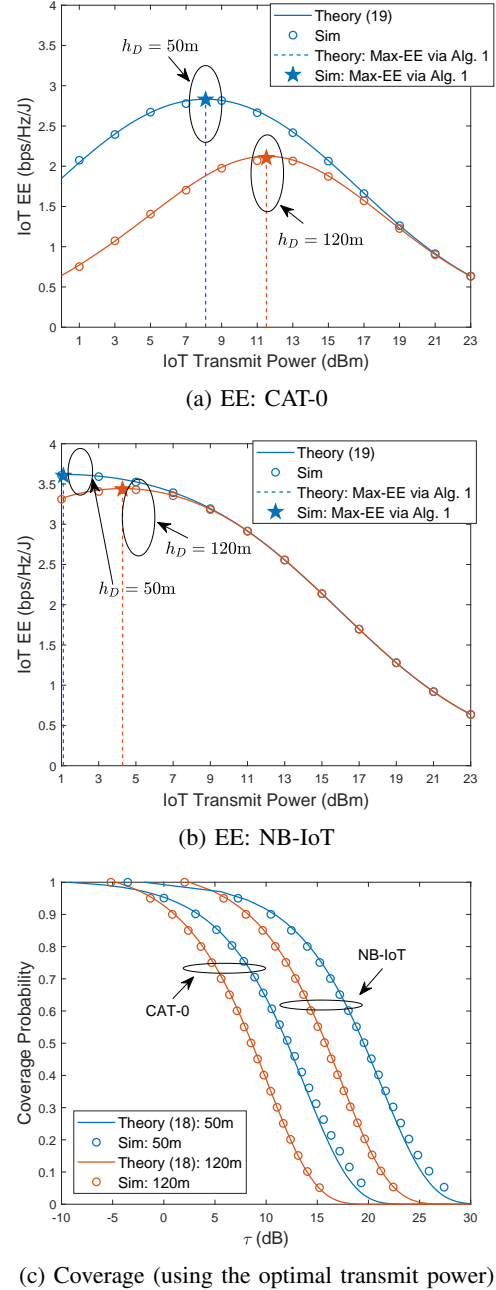
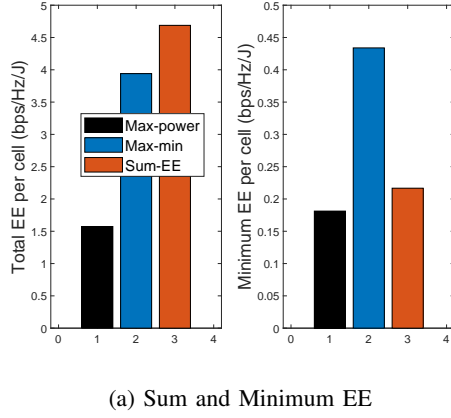


Fig. 4: Validation of the theoretical EE and coverage.

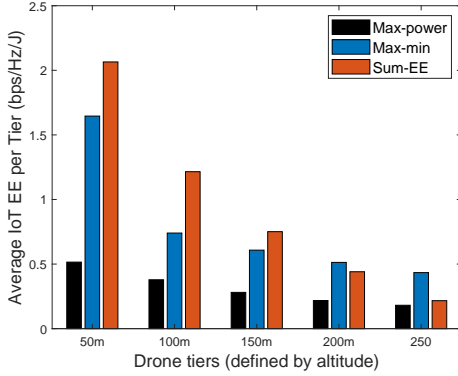
altitude as this tier achieves the lowest EE. In contrast, the *Sum-EE* formulation favors the drones with lower altitudes as they provide higher EE for IoT devices.

#### B. Performance comparison with existing protocols

In this section, we compare the performance of the proposed protocol with existing ones in large networks, and hence the results are obtained via Monte Carlo simulations. We also show the performance of UEs in the absence of IoT devices as a benchmark. For the proposed protocol, we consider two schemes: *Max-EE* using the SC-SD framework (Alg. 1), and *Max-EE* using exhaustive search, where we use extensive network simulations to search for the optimal power. To highlight



(a) Sum and Minimum EE

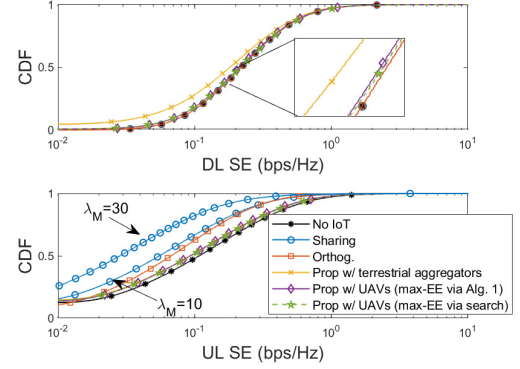


(b) Average EE per drone tier (defined by altitude)

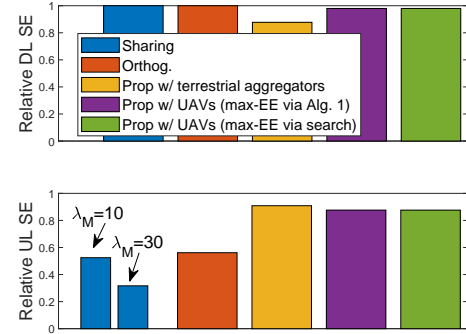
Fig. 5: EE performance for different schemes in the SC-MD case (CAT-0 parameters and  $\rho_{dB} = -12dB$ ).

the benefits of using UAVs, we also consider the proposed protocol with max-power and terrestrial aggregators, e.g., small cells are deployed at the centroid of the clusters instead of UAVs. We assume  $\lambda_U = 50\lambda_B$  and  $\lambda_{CI} = \lambda_D = 5\lambda_B$ . Unless otherwise stated, we consider  $\delta = 1$ ,  $W_U = 0.5W$ , and  $h_D = 50m$ . We show the results assuming CAT-0 IoT devices (similar trends are observed for NB-IoT and hence omitted).

1) *UE performance comparison:* We first study the performance of the UE in the DL and the UL under different protocols. We note that both the orthogonal-based and the proposed protocols decouple the UE UL performance from the IoT density as in the former IoT devices use different frequency blocks, and in the latter IoT devices connect to drones instead of BSs. This is not the case for the sharing-based protocol, where we study the UE's performance for  $\lambda_M = 10$  and  $\lambda_M = 30$ . Fig. 6a shows the distribution of the SE performance across all UEs and Fig. 6b shows the mean SE relative to the benchmark, i.e., the ratio of the mean SE under the given protocol to the mean SE in the absence of IoT devices. Since our model considers IoT devices to only operate in the UL, the DL SE of sharing-based and orthogonal-based protocols is the same as the benchmark. For the proposed protocol, it is shown that the DL degradation is minimal when UAVs are used and the transmit power is optimized to limit the IoT interference. More importantly, the proposed protocols outperform existing ones in the UL, e.g., the relative mean UL



(a) Distribution of the SE



(b) Mean SE relative to the benchmark

Fig. 6: UE DL and UL performance for the different protocols.

SE of the proposed protocols is 1.5x and 2.7x the orthogonal-based and sharing-based ( $\lambda_M = 30$ ) protocols, respectively. This follows due to the resource splitting in the orthogonal-based protocol and the high congestion in the sharing-based one.

2) *IoT performance comparison:* We then study the EE of the IoT device under the different protocols. In Fig. 7a, the EE is shown for different densities of IoT devices. As expected, as the number of IoT devices increases, the EE decreases under all protocols. Yet, the proposed protocol achieves the highest EE and scales better with  $\lambda_M$  compared to existing ones. It is also observed that it is beneficial to use UAVs over terrestrial aggregators as the former provides higher LOS, i.e., the EE improves by 3x when aerial aggregators are used instead of terrestrial ones. In Fig. 7b, we study the EE for different drone's altitudes. We show the performance under the existing protocols and the proposed one with terrestrial aggregators, which do not depend on  $h_D$ , for reference. It is observed that the proposed protocol is beneficial for lower altitudes. At very high altitudes, the received signal power is lower, and the LOS probability with interfering BSs, from different cells, increases. We note that in many regions, e.g., North America, Europe, China, etc., the maximum legal altitude for drones is roughly 120m (400ft), and thus the proposed solution is superior in practical scenarios.

3) *Impact of ACB and resource splitting:* Fig. 8 shows the IoT EE versus the UE SE in the UL under different ACB

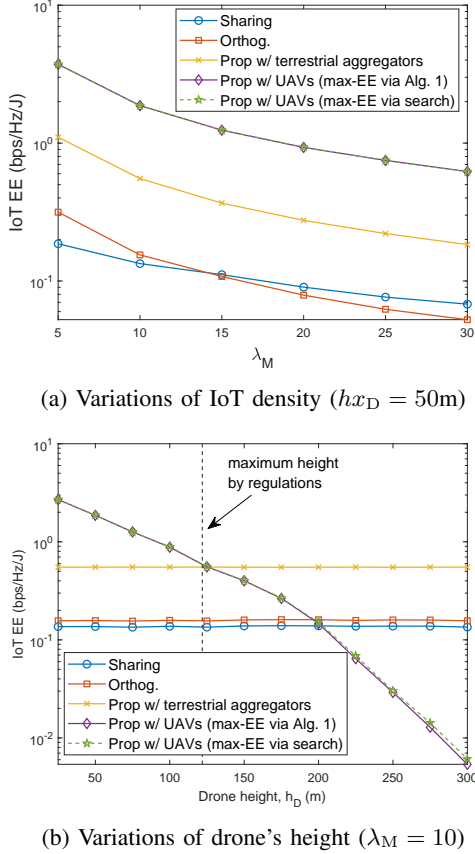


Fig. 7: IoT EE performance under different protocols.

thresholds  $\kappa$  (Fig. 8a) and different frequency allocation ratios  $W_U$  (Fig. 8b). The performance of the proposed protocol, which does not depend on these parameters, is also shown for reference. It can be seen that existing protocols have operating points with higher UE SE performance in comparison with proposed ones. However, high ACB threshold and frequency partitioning ratio are needed, and thus the IoT device will be limited with time and frequency resources, respectively. Finally, it is shown the SC-SD framework leads to a nearly identical performance to exhaustive search, yet the latter requires extensive simulations to solve.

### C. IoT device lifetime comparison

In this section, we show that the EE improvements are translated into extended battery lifetime. To this end, we follow the 3GPP evaluation methodology to compute the lifetime of IoT devices for the different schemes [29], [45]. In particular, the IoT device sends  $N_{\text{rep}}$  reports per day to the network. For each report, the device operates in the following stages: standby, idle, transmission, and reception. Let  $P_S$ ,  $P_I$ , and  $P_{RX}$  denote the power consumption of the standby, idle, and reception stages. Similarly, let  $T_S$ ,  $T_I$ , and  $T_{RX}$  be their durations. For a fair comparison, we assume the energies consumed for these three stages are the same across the schemes, i.e., the schemes only differ in the energy consumed

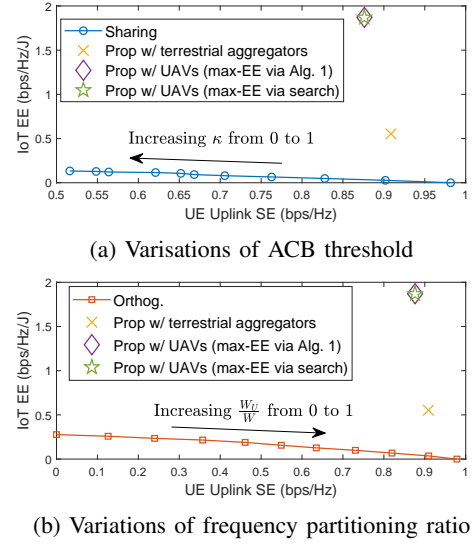


Fig. 8: IoT energy-efficiency vs. UE spectral efficiency ( $\lambda_M = 10$  and  $h_D = 50\text{m}$ ).

during the transmission stage as our focus is on the UL. The transmission duration is

$$T_{\text{TX}}^{(\nu)} = \frac{B/\beta_M^{(\nu)}}{\sum_{k=1}^{K_M} \log_2(1 + \tau_{M,k}) \mathbf{1}(\tau_{M,k+1} \geq \gamma_M^{(\nu)} \geq \tau_{M,k})}, \quad (28)$$

where  $B$  is the total size of the data transmitted per report, which includes the connection request, the data packet, and the acknowledgment [29, Table 4]. The superscript  $\nu$  denotes the scheme used. Similarly,  $P_{\text{TX}}^{(\nu)} = P_{\text{CP}} + \eta^{-1} P_M^{(\nu)}$ . Thus, the total energy consumed per day is given as [29]

$$E_{\text{IoT}}^{(\nu)} = N_{\text{rep}} \left( T_{\text{TX}}^{(\nu)} P_{\text{TX}}^{(\nu)} + T_{\text{RX}} P_{\text{RX}} + T_I P_I \right) + T_S P_S. \quad (29)$$

Let the IoT battery's capacity be  $C_{\text{IoT}}$  Wh, then the device lifetime in years is given as  $Y^{(\nu)} = \frac{C_{\text{IoT}}}{E_{\text{IoT}}^{(\nu)}} \times \frac{3600}{365}$ . Note that increasing the IoT transmit power is expected to improve the SINR, increasing the rate and decreasing  $T_{\text{TX}}^{(\nu)}$ . Yet, this comes at the expense of increased power consumption during the transmission stage, i.e., higher  $P_{\text{TX}}^{(\nu)}$ .

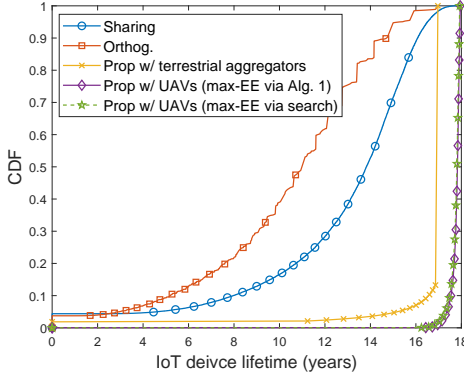
Using the parameters given in Table II [29], Fig. 9 shows the CDF of the IoT device lifetime for each scheme. We have two observations. First, the improvements in EE under the proposed scheme are translated into tangible enhancements to the IoT device lifetime, e.g., the median lifetime is increased by more than four and six years compared to sharing and orthogonal-based schemes, respectively. Second, due to the aggregators' proximity to IoT devices, the variance in lifetime across devices is lower under the proposed schemes. When UAVs are used instead of terrestrial aggregators, the variance is further reduced thanks to the better LOS conditions, where it is shown that almost all devices have a lifetime of +16 years.

## VI. CONCLUSIONS

In this work, we have proposed a TDD protocol for a shared spectrum access between massive IoT and cellular UEs with UAVs acting as data aggregators. Using stochastic geometry,

TABLE II: Battery lifetime parameters [5], [29]

Description	Parameters
IoT device	NB-IoT with $W = 180\text{KHz}$ , $C_{\text{IoT}} = 5\text{Wh}$ $B = 229\text{bytes}$ [29, Table 4], and $N_{\text{rep}} = 12$
Powers	$P_{\text{RX}} = 90\text{mW}$ , $P_{\text{I}} = 3\text{mW}$ , and $P_{\text{S}} = 0.015\text{mW}$ [29, Table 1]
Durations	$T_{\text{RX}} = 565\text{ms}$ , $T_{\text{I}} = 22451\text{ms}$ , and $T_{\text{S}} = 86400\text{s}$ [29, Table 6]

Fig. 9: Distribution of IoT device lifetime ( $h_D = 50\text{m}$ ).

it is shown that the protocol improves the average allocated resources of IoT devices and UEs compared to resource splitting and ACB, yet UEs experience additional interference from IoT devices. Thus, we have optimized the transmit power of the IoT device to maximize its energy-efficiency while constraining the interference on UEs. The proposed algorithms aim to provide a single transmit power value per cluster of IoT devices, reducing the computational complexity and limiting the control overhead. The analysis of the stochastic optimization framework is validated via simulations for the single-cell case. For larger networks, Monte Carlo simulations have shown that the proposed system significantly improves the EE, and hence the IoT device lifetime, with minimal degradation on the UE spectral-efficiency.

The key insights gleaned from this work are as follows. First, it is beneficial for drones to fly at lower altitudes as higher altitudes increase the LOS with interferers, forcing the IoT device to increase its transmit power to combat coverage degradation, which eventually affects its EE. In case drones, belonging to the same BS, fly at different altitudes, then maximizing the minimum EE and the total EE amount to prioritizing devices connected to drones at the highest and the lowest altitudes, respectively. Second, the extended coverage mode, where IoT devices transmit at maximum power, is not necessarily energy efficient as the gain in coverage does not outweigh the loss in power consumption.

## APPENDIX

### A. Proof of Theorem 1

Recall that the aggregate interference at the UE is given as

$$I_U = \underbrace{\sum_{y_b \in \Phi'_B} f_b y_b^{-\alpha_G}}_{I_{U,B}} + \underbrace{\sum_{z_m \in \Phi'_M} \frac{P_M}{P_B/U_B} f_m z_m^{-\alpha_G}}_{I_{U,M}}, \quad (30)$$

where we have normalized the interference by  $L_0 P_B / U_B$ . Using the Gil-Pelaez Inversion theorem [40] to evaluate the interference CDF, we get  $F_{I_U}(\frac{q_B}{\tau x^{\alpha_G}}) = \frac{1}{2} - \frac{1}{\pi} \int_0^\infty \text{Im} \{ \varphi_{I_U}(x^{\alpha_G} t) e^{-j t q_B / \tau} \} dt$ , where  $\varphi_{I_U}(x^{\alpha_G} t) = \mathbb{E}_{I_U}[\exp(j t x^{\alpha_G} I_U)]$  is the characteristic function (CF), which is given as

$$\varphi_{I_U}(x^{\alpha_G} t) \stackrel{(a)}{=} \mathbb{E}_{I_{U,B}} \left[ \exp \left( j t x^{\alpha_G} \sum_{y_b \in \Phi'_B} f_b y_b^{-\alpha_G} \right) \right] \times \mathbb{E}_{I_{U,M}} \left[ \exp \left( j t x^{\alpha_G} \sum_{z_m \in \Phi'_M} \frac{P_M}{P_B/U_B} f_m z_m^{-\alpha_G} \right) \right], \quad (31)$$

where (a) follows since interfering BSs are independent from the interfering IoT devices. Using the probability-generating functional of the HPPP process [28], it can be shown that  $\varphi_{I_{U,B}}(x^{\alpha_G} t) = \exp(\pi \lambda_B x^2 (1 - \mathbb{E}_{f_b}[\Omega(f_b, \delta_G, t)]))$ , where  $\Omega(f_b, \delta_G, t) = {}_1F_1(-\delta_G; 1 - \delta_G; j t f_b)$ , and  ${}_1F_1(a; b; c)$  is the confluent hypergeometric function [46]. Similarly, we have

$$\begin{aligned} \varphi_{I_{U,M}}(x^{\alpha_G} t) &\stackrel{(a)}{=} e^{-2\pi \lambda_D \int_0^\infty y \left( 1 - \mathbb{E}_{f_m} \left[ e^{j t \frac{U_B P_M f_m x^{\alpha_G}}{P_B y^{\alpha_G}}} \right] \right) dy} \\ &\stackrel{(b)}{=} e^{-\delta_G \pi \lambda_D x^2 \int_0^\infty l^{-(1+\delta_G)} \left( 1 - \frac{1}{1 - j t l \frac{P_M}{P_B/U_B}} \right) dl} \\ &= \exp \left( -\pi \lambda_D x^2 \hat{P}_{B,M}^{\delta_G} (-j t)^{\delta_G} \right), \end{aligned} \quad (32)$$

where (a) follows using the fact that the set of interfering IoT devices can be modeled as a set of Poisson interferers with density of  $\lambda_D$  as one IoT device is scheduled per drone per time-frequency slot, and (b) follows using the CF of  $f_m$  and then using the substitution  $l = x^{\alpha_G} y^{-\alpha_G}$ . Here, the integral lower limit is zero as the set of interfering IoT devices is independent of the UE's location, i.e., no protection zone is present unlike the case of interfering BSs which cannot be closer than the tagged BS. To summarize, we have  $\varphi_{I_U}(x^{\alpha_G} t) = \exp \left( \pi \lambda_B x^2 \left( 1 - \mathbb{E}_f[\Omega(f_b, \delta_G, t)] - (\lambda_D / \lambda_B) \hat{P}_{B,M}^{\delta_G} (-j t)^{\delta_G} \right) \right)$ . Thus, the coverage becomes

$$\mathbb{C}_{U,DL}^P(\tau) = \frac{1}{2} - 2\lambda_B \int_0^\infty \frac{1}{t} \text{Im} \{ \varphi_g(-t/\tau) \Xi(t) \} dt, \quad (33)$$

where  $\varphi_{g_B}(-t/\tau) = (1 + j t / \tau)^{-\Delta_B}$  is the CF of  $g_B$  and

$$\begin{aligned} \Xi(t) &= \int_0^\infty x e^{-\pi \lambda_B x^2 \left( \mathbb{E}_f[\Omega(f_b, \delta_G, t)] + (\lambda_D / \lambda_B) \hat{P}_{B,M}^{\delta_G} (-j t)^{\delta_G} \right)} dx \\ &= \frac{(2\pi \lambda_B)^{-1}}{\mathbb{E}_f[\Omega(f_b, \delta_G, t)] + (\lambda_D / \lambda_B) \hat{P}_{B,M}^{\delta_G} (-j t)^{\delta_G}}. \end{aligned} \quad (34)$$

Plugging (34) in (33) and using  $\mathbb{E}_f[\Omega(f_b, \delta_G, t)] = {}_2F_1(\Psi_G, U_B; 1 - \delta_G; j t)$ , we arrive at (11).

### B. Proof of Proposition 1

Let the IoT device be at a distance  $x_M$  from the drone. Then, the received signal power at the drone is given as

$$\begin{aligned} & \mathbb{P}(S_M \leq \tau) \\ & \stackrel{(a)}{\approx} \mathbb{P}(P_M L_M x_M^{-\alpha_A} \leq \tau) \\ & = 1 - F_{x_M} \left( \left( \frac{P_M L_M}{\tau} \right)^{1/\alpha_A} \right) \\ & \stackrel{(b)}{=} \begin{cases} 1 - \frac{(P_M L_M / \tau)^{\delta_A} - h_D^2}{R^2}, & \frac{P_M L_M}{(R^2 + h_D^2)^{1/\delta_A}} \leq \tau \leq \frac{P_M L_M}{h_D^{1/\delta_A}} \\ 0, & \text{otherwise} \end{cases}, \end{aligned} \quad (35)$$

where (a) follows by using the mean LOS probability instead of the actual one, and (b) follows using the CDF of the distance between the typical IoT device and the drone  $F_{x_M}(\cdot)$ , which can be found using the fact that the IoT device is randomly distributed over an area of radius  $R$  centered around the 2D coordinates of the drone. Similarly, let  $r_B$  denote the distance between the tagged BS and the drone, then  $\mathbb{P}(I_B \leq \tau) \approx \mathbb{P}(P_B L_B r_B^{-\alpha_A} \leq \tau) = 1 - F_{r_B} \left( \left( \frac{P_B L_B}{\tau} \right)^{1/\alpha_A} \right)$ . Recall that the distance between a point in  $\mathbb{R}^2$  and the nearest BS is distributed as  $f_{y_B}(y) = 2\pi\lambda_B y \exp(-2\pi\lambda_B y^2)$  [36]. Thus, the distribution of  $r_B = \sqrt{y_B^2 + h_D^2}$  can be shown to be  $f_{r_B}(r) = \frac{2rf_{y_B}(\sqrt{r^2 - h_D^2})}{\sqrt{r^2 - h_D^2}}$ . Thus, we can compute  $F_{r_B}(r) = \int_{h_D}^{\infty} f_{r_B}(r) dr$  to arrive at (17).

### C. Proof of Proposition 2

We first derive useful properties for  $r(p)$ . In particular,  $r(p)$  is a non-negative sum of coverage probabilities, each is non-decreasing with the transmit power, and thus  $r(p)$  is non-decreasing with  $p$ . Thus, the  $t$ -sublevel sets, i.e.,  $\mathcal{R}_{t,\text{sub}} = \{p | r(p) \leq t\}$ , and the  $t$ -superlevel sets, i.e.,  $\mathcal{R}_{t,\text{sup}} = \{p | r(p) \geq t\}$ , are convex, and hence  $r(p)$  is quasilinear [42]. To show that  $r(p)$  is S-shaped, we take the 2nd derivative with respect to  $p$  to get

$$\begin{aligned} \frac{d^2 r(p)}{dp^2} &= \delta_A \pi \lambda_B \tilde{L}_M^2 (P_B L_B)^{\delta_A} \sum_{k=1}^{K_M} \frac{\mu_k e^{-\pi \lambda_B \left( \frac{p \tilde{L}_M - P_N}{P_B L_B} \right)^{\delta_A}}}{\tau_{M,k}^2 \left( \frac{p \tilde{L}_M}{\tau_{M,k}} - P_N \right)^{2(1+\delta_A)}} \\ &\quad \times \left\{ \delta_A \pi \lambda_B (P_B L_B)^{\delta_A} - (1 + \delta_A) \left( \frac{p \tilde{L}_M}{\tau_{M,k}} - P_N \right)^{\delta_A} \right\}. \end{aligned} \quad (36)$$

Note that  $\left( \frac{p \tilde{L}_M - P_N}{P_B L_B} \right) \geq 0$  for any feasible  $\tau_{M,k}$  and the derivative is non-increasing with  $p$ . Furthermore, there exists a point  $p^\bullet$  such that  $\frac{d^2 r(p)}{dp^2} \geq 0$  for  $p \leq p^\bullet$  and  $\frac{d^2 r(p)}{dp^2} \leq 0$  for  $p \geq p^\bullet$ , and hence the function is S-shaped. To prove that  $r(p)$  is concave when the condition in (23) holds, it is sufficient to show that the coverage  $\mathbb{P}(\hat{\gamma}_M \geq \tau_k)$  is concave in  $p$  as  $r(p)$  is a non-negative sum of the coverage probabilities. This can be shown by taking the second derivative of the coverage and showing that it is non-positive if and only if

$$\delta_A \pi \lambda_B (P_B L_B)^{\delta_A} - (1 + \delta_A) \left( \frac{p \tilde{L}_M}{\tau_k} - P_N \right)^{\delta_A} \leq 0, \quad (37)$$

which is satisfied when the condition in (23) holds.

To prove that the objective function in (22) is quasiconcave, then it is sufficient to prove that the superlevel sets  $\mathcal{E}_{t,\text{sup}} = \{p | \frac{r(p)}{c(p)} \geq t\}$  are convex. Note since the objective is non-negative, then we only need to consider the case for  $t \geq 0$  and prove that  $\{p | r(p) - c(p)t \geq 0\}$  is convex. We consider two cases. First, for  $p \geq p^\bullet$ ,  $r(p)$  is concave, and thus for  $p_1, p_2 \in \mathcal{E}_{t,\text{sup}}$  and  $\beta \in [0, 1]$  we have

$$\begin{aligned} & r(\beta p_1 + (1 - \beta)p_2) - c(\beta p_1 + (1 - \beta)p_2)t \\ & \stackrel{(a)}{\geq} \beta r(p_1) + (1 - \beta)r(p_2) - c(\beta p_1 + (1 - \beta)p_2)t \\ & \stackrel{(b)}{=} \beta (r(p_1) - c(p_1)t) + (1 - \beta)(r(p_2) - c(p_2)t) \\ & \geq 0, \end{aligned} \quad (38)$$

where (a) follows because  $r(p)$  is concave and (b) follows because  $c(p)$  is affine, and thus,  $\mathcal{E}_{t,\text{sup}}$  is convex. Second, for  $p \leq p^\bullet$ ,  $r(p)$  is convex. Taking the first derivative of  $\bar{E}(p)$ , we get

$$\frac{d\bar{E}(p)}{dp} = \frac{\eta^{-1}(pr'(p) - r(p)) + P_{CP}r'(p)}{c^2(p)}. \quad (39)$$

The second sum term  $r'(p) \geq 0$  as  $r(p)$  is a non-decreasing function in  $p$ . In addition, the first sum term  $pr'(p) - r(p) \geq 0$  because  $r(p)$  is convex, i.e., for any convex differentiable function  $g(x)$  with  $g(0) = 0$ , we have  $g(y) \geq g(x) + (y - x)g'(x)$  [42], and by setting  $y = 0$  we get  $xg'(x) \geq g(x)$ . Thus, the derivative is non-negative, i.e., it is a non-decreasing function in  $p \leq p^\bullet$ , and hence the superlevel sets are convex, which completes the proof that the objective function is quasiconcave. To prove that the objective function is unimodal, note that  $\bar{E}(0) = \bar{E}(\infty) = 0$ , and since  $\bar{E}(p)$  is quasiconcave, then it has to be unimodal.

### REFERENCES

- [1] G. Hattab and D. Cabric, "Energy-efficient massive cellular IoT shared spectrum access via mobile data aggregators," in *IEEE 13th Int. Conf. Wireless and Mobile Computing (WiMob)*, Oct. 2017, pp. 1–6.
- [2] ITU-R, "IMT Vision – framework and overall objectives of the future development of IMT for 2020 and beyond," ITU-R, M. 2083-0, Sep. 2015.
- [3] McKinsey Global Institute, "The internet of things: Mapping the value beyond the hype," McKinsey & Company, Tech. Rep., Jun. 2015.
- [4] Z. Dawy, W. Saad, A. Ghosh *et al.*, "Toward massive machine type cellular communications," *IEEE Wireless Commun.*, vol. 24, no. 1, pp. 120–128, Feb. 2017.
- [5] 3GPP, "Cellular system support for ultra low complexity and low throughput internet of things, release 13," TS 45.820, Nov. 2015.
- [6] A. Rico-Alvarino, M. Vajapeyam, H. Xu *et al.*, "An overview of 3GPP enhancements on machine to machine communications," *IEEE Commun. Mag.*, vol. 54, no. 6, pp. 14–21, Jun. 2016.
- [7] E. Soltanmohammadi, K. Ghavami, and M. Naraghi-Pour, "A survey of traffic issues in machine-to-machine communications over LTE," *IEEE Internet Things J.*, vol. 3, no. 6, pp. 865–884, Dec. 2016.
- [8] A. Laya, L. Alonso, and J. Alonso-Zarate, "Is the random access channel of LTE and LTE-A suitable for M2M communications? a survey of alternatives," *Commun. Surveys Tuts.*, vol. 16, no. 1, pp. 4–16, 2014.
- [9] P. K. Wali, A. A. N., and D. Das, "Optimal time-spatial randomization techniques for energy efficient IoT access in LTE-advanced," *IEEE Trans. Veh. Technol.*, vol. 66, no. 8, pp. 7346–7359, Aug. 2017.
- [10] Z. Feng, Z. Feng, and T. A. Gulliver, "Biologically inspired two-stage resource management for machine-type communications in cellular networks," *IEEE Trans. Wireless Commun.*, vol. 16, no. 9, pp. 5897–5910, Sep. 2017.



- [11] N. Jiang, Y. Deng, A. Nallanathan *et al.*, "Analyzing random access collisions in massive IoT networks," *IEEE Trans. Wireless Commun.*, vol. 17, no. 10, pp. 6853–6870, Oct. 2018.
- [12] Z. Wang and V. W. S. Wong, "Optimal access class barring for stationary machine type communication devices with timing advance information," *IEEE Trans. Wireless Commun.*, vol. 14, no. 10, pp. 5374–5387, Oct. 2015.
- [13] F. Morvari and A. Ghasemi, "Two-stage resource allocation for random access M2M communications in LTE network," *IEEE Commun. Lett.*, vol. 20, no. 5, pp. 982–985, May 2016.
- [14] T. Kwon and J. M. Cioffi, "Random deployment of data collectors for serving randomly-located sensors," *IEEE Trans. Wireless Commun.*, vol. 12, no. 6, pp. 2556–2565, Jun. 2013.
- [15] D. Malak, H. S. Dhillon, and J. G. Andrews, "Optimizing data aggregation for uplink machine-to-machine communication networks," *IEEE Trans. Commun.*, vol. 64, no. 3, pp. 1274–1290, Mar. 2016.
- [16] U. Tefek and T. J. Lim, "Relaying and radio resource partitioning for machine-type communications in cellular networks," *IEEE Trans. Wireless Commun.*, vol. 16, no. 2, pp. 1344–1356, Feb. 2017.
- [17] J. Guo, S. Durrani, X. Zhou *et al.*, "Massive machine type communication with data aggregation and resource scheduling," *IEEE Trans. Commun.*, vol. 65, no. 9, pp. 4012–4026, Sep. 2017.
- [18] 3GPP, "Study on enhanced LTE support for aerial vehicles," TR 36.777, Dec. 2017.
- [19] I. Bor-Yaliniz and H. Yanikomeroglu, "The new frontier in RAN heterogeneity: Multi-tier drone-cells," *IEEE Commun. Mag.*, vol. 54, no. 11, pp. 48–55, Nov. 2016.
- [20] H. Menouar, I. Guvenc, K. Akkaya *et al.*, "UAV-enabled intelligent transportation systems for the smart city: Applications and challenges," *IEEE Commun. Mag.*, vol. 55, no. 3, pp. 22–28, Mar. 2017.
- [21] Z. Yuan, J. Jin, J. Chen *et al.*, "ComProSe: Shaping future public safety communities with prose-based UAVs," *IEEE Commun. Mag.*, vol. 55, no. 12, pp. 165–171, Dec. 2017.
- [22] N. H. Motlagh, M. Bagaa, and T. Taleb, "UAV-based IoT platform: A crowd surveillance use case," *IEEE Commun. Mag.*, vol. 55, no. 2, pp. 128–134, Feb. 2017.
- [23] Z. Yuan, J. Jin, L. Sun *et al.*, "Ultra-reliable IoT communications with UAVs: A swarm use case," *IEEE Commun. Mag.*, vol. 56, no. 12, pp. 90–96, Dec. 2018.
- [24] Y. Zeng, R. Zhang, and T. J. Lim, "Throughput maximization for UAV-enabled mobile relaying systems," *IEEE Trans. Commun.*, vol. 64, no. 12, pp. 4983–4996, Dec. 2016.
- [25] O. M. Bushnaq, A. Celik, H. ElSawy *et al.*, "Aeronautical data aggregation and field estimation in IoT networks: Hovering & traveling time dilemma of uavs," *arXiv preprint arXiv:1810.08035*, Oct. 2018.
- [26] C. Zhan, Y. Zeng, and R. Zhang, "Energy-efficient data collection in UAV enabled wireless sensor network," *IEEE Wireless Commun. Lett.*, vol. 7, no. 3, pp. 328–331, Jun. 2018.
- [27] M. Mozaffari, W. Saad, M. Bennis *et al.*, "Mobile unmanned aerial vehicles (UAVs) for energy-efficient internet of things communications," *IEEE Trans. Wireless Commun.*, vol. 16, no. 11, pp. 7574–7589, Nov. 2017.
- [28] M. Haenggi, *Stochastic Geometry for Wireless Networks*. Cambridge University Press, 2012.
- [29] 3GPP, "NB-IoT: Battery lifetime evaluation," R1-156006, Oct. 2015.
- [30] L. H. Afify, H. ElSawy, T. Y. Al-Naffouri *et al.*, "A unified stochastic geometry model for MIMO cellular networks with retransmissions," *IEEE Trans. Wireless Commun.*, vol. 15, no. 12, pp. 8595–8609, Dec. 2016.
- [31] Y. Zeng and R. Zhang, "Energy-efficient UAV communication with trajectory optimization," *IEEE Trans. Wireless Commun.*, vol. 16, no. 6, pp. 3747–3760, Jun. 2017.
- [32] M. Mozaffari, W. Saad, M. Bennis *et al.*, "Unmanned aerial vehicle with underlaid device-to-device communications: Performance and tradeoffs," *IEEE Trans. Wireless Commun.*, vol. 15, no. 6, pp. 3949–3963, Jun. 2016.
- [33] A. Al-Hourani, S. Kandeepan, and S. Lardner, "Optimal LAP altitude for maximum coverage," *IEEE Wireless Commun. Lett.*, vol. 3, no. 6, pp. 569–572, Dec. 2014.
- [34] 3GPP, "Study on 3D channel model for LTE," TR 36.889, May 2017.
- [35] W. Bao and B. Liang, "Rate maximization through structured spectrum allocation and user association in heterogeneous cellular networks," *IEEE Trans. Commun.*, vol. 63, no. 11, pp. 4510–4524, Nov. 2015.
- [36] Y. Lin, W. Bao, W. Yu *et al.*, "Optimizing user association and spectrum allocation in HetNets: A utility perspective," *IEEE J. Sel. Areas Commun.*, vol. 33, no. 6, pp. 1025–1039, Jun. 2015.
- [37] A. Zappone, L. Sanguinetti, G. Bacci *et al.*, "Energy-efficient power control: A look at 5G wireless technologies," *IEEE Trans. Signal Process.*, vol. 64, no. 7, pp. 1668–1683, Apr. 2016.
- [38] W. Mei, Q. Wu, and R. Zhang, "Cellular-connected UAV: Uplink association, power control and interference coordination," *arXiv preprint arXiv:1807.08218*, Jul. 2018.
- [39] A. Biazon, C. Pielli, A. Zanella *et al.*, "On the energy/distortion tradeoff in the IoT," *arXiv preprint arXiv:1702.03695*, Feb. 2017.
- [40] J. Gil-Pelaez, "Note on the inversion theorem," *Biometrika*, vol. 38, no. 3-4, Dec. 1951.
- [41] H. Wei, N. Deng, W. Zhou *et al.*, "Approximate SIR analysis in general heterogeneous cellular networks," *IEEE Trans. Commun.*, vol. 64, no. 3, pp. 1259–1273, Mar. 2016.
- [42] S. Boyd and L. Vandenberghe, *Convex Optimization*. Cambridge University Press, 2004.
- [43] J.-P. Crouzeix and J. A. Ferland, "Algorithms for generalized fractional programming," *Mathematical Programming*, vol. 52, no. 1, pp. 191–207, 1991.
- [44] S. Schaible and J. Shi, "Fractional programming: the sum-of-ratios case," *Optimization Methods and Software*, vol. 18, no. 2, pp. 219–229, 2003.
- [45] G. Hattab and D. Cabric, "Performance analysis of uplink cellular IoT using different deployments of data aggregators," in *Proc. IEEE Global Communications Conf. (GLOBECOM)*, Dec. 2018, pp. 1–6.
- [46] A. Jeffrey and D. Zwillinger, *Table of Integrals, Series, and Products*. Elsevier LTD, Oxford, 2014.